
Open Archive TOULOUSE Archive Ouverte (OATAO)
OATAO is an open access repository that collects the work of Toulouse researchers and makes it freely available over the web where possible.

This is an author-deposited version published in : http://oatao.univ-toulouse.fr/
Eprints ID : 13080

**To link to this article** : DOI :10.1109/ULTSYM.2014.0264
URL : http://dx.doi.org/10.1109/ULTSYM.2014.0264

**To cite this version** : Szasz, Teodora and Basarab, Adrian and Vaida, Mircea-Florin and Kouamé, Denis *Beamforming with sparse prior in ultrasound medical imaging*. (2014) In: IEEE International Ultrasonics Symposium - IUS 2014, 3 September 2014 - 6 September 2014 (Chicago, United States).

Any correspondance concerning this service should be sent to the repository administrator: staff-oatao@listes-diff.inp-toulouse.fr

# Beamforming with sparse prior in ultrasound medical imaging

Teodora Szasz*, Adrian Basarab*, Mircea-Florin Vaida†, and Denis Kouamé*
*Université de Toulouse, IRIT, UMR CNRS 5505, France
†Technical University of Cluj-Napoca, Romania
Email: teodora.szasz@irit.fr

***Abstract*—Nowadays the classical Delay-and-Sum (DAS) beamformer is extensively used in ultrasound imaging due to its low computational characteristics. However, it suffers from high sidelobe level, poor resolution and low contrast. An alternative is the Minimum-Variance (MV) beamformer which results in a higher image quality both in terms of spatial resolution and contrast. Even so, these benefits come at the expense of a higher computation complexity that limits its real-time capabilities. One solution that recently gained noticeable interest is the exploit of the sparsity of the scanned medium. Based on this assumption, we extend the DAS method to yield sparse results by using the Bayesian Information Criterion (BIC). Our realistic simulations demonstrate that the proposed beamforming (BF) method shows better performance than the classical DAS and MV in terms of lateral resolution, sidelobe reduction and contrast.**

***Index Terms*—Adaptive beamforming, Bayesian Information Criterion, sparse prior, synthetic aperture imaging.**

## I. Introduction

ULTRASOUND (US) medical imaging is widely used nowadays because of its safety, low cost and real-time characteristics. Beamforming plays a major role in medical US imaging, allowing the spatial selectivity of the signal in transmission/reception [1]. In reception, it steers and focus the received echoes in a desired direction to detect tissue structures. The BF methods can be classified as either data-independent or data-dependent, following the type of weights applied to the array output. Even if classical delay-and-sum beamformer is data-independent, it is currently widely used by the most commercial ultrasound scanners, because of its simplicity and real-time capabilities. Its aim is to delay the signals received by the sensors (raw signals), to weight them using fixed weights and subsequently sum the signals from individual sensors in order to form one radiofrequency (RF) line. Capon BF [2], called Minimum-Variance BF in US imaging [3], is a data-dependent beamformer whose aim is to improve the contrast and the lateral resolution of DAS. The main idea of MV BF is to adaptively weight the received RF focused data prior of summing them. The weights are computed from the analysis of the signals corresponding to the point of interest over several "observations" of that point, such that they minimize the beamformer output power while maintaining unity gain in the focus direction. Despite the resolution and the interference suppression capability of MV, its computation complexity is higher than that of DAS, which limits its real-time capabilities. There has been growing interest in lowering the computational complexity of MV. Zeng *et al.* [4] and Asl *et al.* [5] reduced the computational complexity of the MV beamformer from $O(L^3)$ to $O(L^2)$.

Recently, the sparse models have gained particular interest in US imaging, as for example in compressive sampling related applications [6]. More specifically, several authors proposed to model the RF signals with sparse priors, e.g. [7]. In [8] Tur *et al.* proposed that the echoes reflected by multiple reflectors, located at some unknown positions, can be modeled as a sum of pulses with known shapes and with unknown amplitudes. Starting from this idea, we are interested in evaluating the use of sparse priors in the BF process, based on a selection criteria inspired from Bayesian Information Criterion (BIC), e.g. [9]. BIC is widely used in speech processing, especially in speaker recognition, where the speakers are sparsely located. In ultrasound imaging we show how this model can be used to sparsify the sources by choosing the goodness of fitness between the raw data and the DAS BF data.

In this paper the BIC criteria was evaluated in the context of US imaging in order to detect the strong reflectors from an US RF image. The results were compared with those obtained by DAS and MV beamformers, showing that the proposed method yields better results in terms of contrast and lateral resolution.

The outline of this paper is as follows: section II introduces briefly the background of BF in US imaging and describes the proposed method (US-BIC). Section III illustrates the results of the proposed method on different simulated data, and compares them with the ones obtained by applying DAS and MV. The conclusions are given in Section IV.

## II. Proposed Method

For a linear transducer of $M$ elements, we consider hereafter the case of a synthetic aperture US imaging, where $M_{act}$ active elements are used in both transmit and receive. The beamformed output with the classical DAS BF can be written as:

$$\hat{\boldsymbol{s}}_i(n) = \sum_{k=1}^{M_{act}} w_k \boldsymbol{y}_k^{(i)}(n - \Delta_k(n)), \quad \begin{array}{l} i = 1, \cdots, M \\ n = 1, \cdots, N, \end{array} \tag{1}$$

where $\boldsymbol{y}_k$ is the $N \times 1$ raw data received by the k-th element of the transducer, $\Delta_k(n)$ is the time delay dependent on the

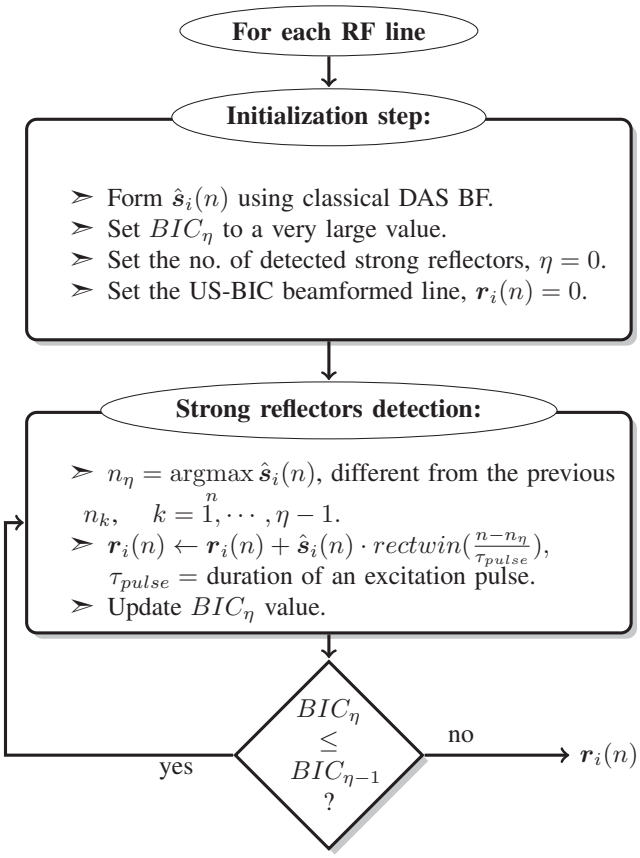


Fig. 1: Flow diagram of the US-BIC BF algorithm.

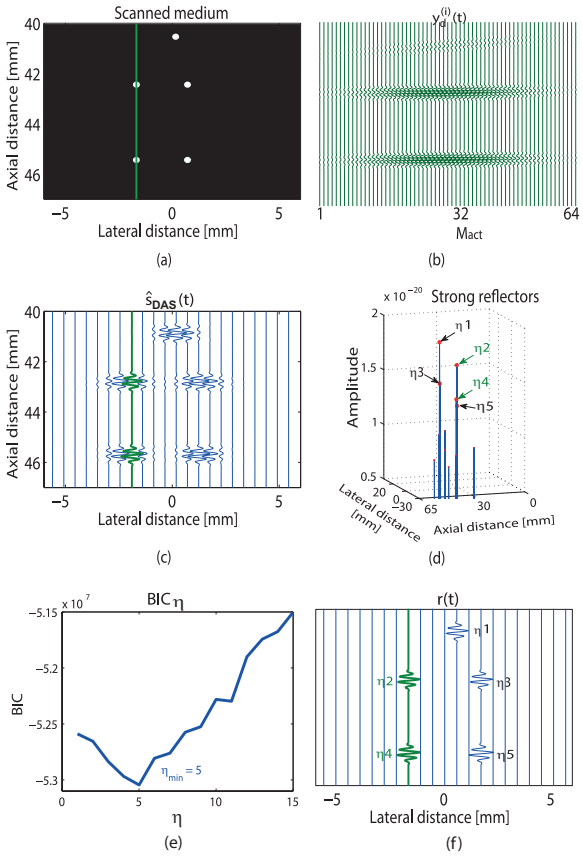


Fig. 2: Strong reflector detection in US-BIC BF: (a) The scanned medium. (b) The raw RF data, $\boldsymbol{y}_d^{(i)}(n)$. (c) The signals obtained after applying DAS BF for all the raw RF data. (d) The distribution of the amplitudes of the RF signals from (c).

distance between the k-th element and the focus point and $w_k$ are the beamformer weights.

We can rewrite Eq. 1 as:

$$\hat{\boldsymbol{s}}_i(n) = \boldsymbol{w}^H(n)\boldsymbol{y}_d^{(i)}(n), \tag{2}$$

where $\boldsymbol{y}_d(n) \in \mathbb{R}^{M\times 1}$, $\boldsymbol{y}_d(n) = \boldsymbol{y}(n - \Delta_k(n))$ is the dynamically focused version of the raw data $\boldsymbol{y}(n) = [y_1^{(i)}(n), \ldots, y_{Mact}^{(i)}(n)]^T$, $\boldsymbol{w}(n) = [w_1, \ldots, w_{Mact}]^T$ is the vector of the beamformer weights, $(\cdot)^T$ and $(\cdot)^H$ represent the transpose and conjugate transpose, respectively.

The aim of the proposed method is to automatically detect the strong reflectors in the RF images by using a US-adapted BIC minimization. As input, we consider the result of DAS method, on which we apply the BIC model selection. The proposed US-BIC BF algorithm is summarized in the Fig. 1.

In the initialization step we consider as input the DAS beamformed RF data, whose equation is given in Eq. 1, we set the BIC to a very large value and we assume that we did not detect any strong reflector, by setting the number of the reflectors, $\eta = 0$ and its retained signal, $\boldsymbol{r}_i(n) = 0$. In the *Strong reflectors detection* step we pick the first most strongest reflector, by means of its amplitude and we extract its signal, $\boldsymbol{r}_i(n)$, from its corresponding DAS beamformed RF line, $\hat{\boldsymbol{s}}_i(n)$. Using the aforementioned data, we therefore calculate the $BIC_\eta$ cost function:

$$BIC_\eta = \overbrace{2MNln(\sum_{i=1}^{M}\sum_{k=1}^{M_{act}} \|\boldsymbol{r}_i(n) - \boldsymbol{y}_d^{(i)}(n)\|_2^2)}^{\text{data attachement}} + \underbrace{\eta\lambda ln(MN)}_{\text{sparsity constrain}}, \tag{3}$$

where $\lambda$ is the hyper-parameter balancing between the data attachment and the sparsity constraint. If $BIC_\eta$ is bigger than the one calculated at the previous iteration, the algorithm stops, we consider that the number of the strong reflectors of the RF line is found, and $\boldsymbol{r}_i(n)$ will be the US-BIC beamformed RF line. Otherwise, we repeat the *Strong reflectors detection* step until $BIC_\eta$ will be higher than the previously calculated one. Briefly, for one RF line, the US-BIC method iteratively estimates $\eta$ by minimizing the $BIC_\eta$ cost function, representing a trade-off (imposed by $\lambda$) between data attachment and the sparsity of the beamformed RF line.

To illustrate our method, we show in Fig. 2 a toy example of a medium containing five point sources placed at different depths and positions (Fig. 2(a)). Supposing that a US probe is

TABLE I: Parameters of Field II simulations

| Transducer | |
|---|---|
| Transducer type | Linear array |
| Transducer element pitch | 231 $\mu$m |
| Transducer element kerf | 38.5 $\mu$m |
| Transducer element height | 14 mm |
| Center frequency, $f_0$ | 4 MHz |
| Sampling frequency, $f_s$ | 40 MHz |
| Speed of sound, $c$ | 1540 m/s |
| Wavelength | 385 $\mu$m |
| Excitation pulse | Two-cycle sinusoidal at $f_0$ |
| **Synthetic Aperture Emission** | |
| Receive Apodization | Hanning |
| Number of transmitting elements | 64 |
| Number of receiving elements | 64 |
| Number of emissions | 204 |

scanning this medium, the RF raw signals $\boldsymbol{y}_d^{(i)}(n)$ received by one element of the probe are shown in Fig. 2(b). If we apply the DAS BF to this set of raw signals, we obtain the DAS beamformed RF lines in Fig. 2(c). The strongest point sources are shown in the Fig. 2(d). Using the flow process of the US-BIC BF method described in the Fig. 1, we show the values of $BIC_\eta$ in Fig. 2(e). We can observe that the minimum value of $BIC_\eta$ is obtained for $\eta = 5$, which represents the exact number of the strong detectors present in the given medium. The final US-BIC beamformed RF lines are illustrated in the Fig. 2(f).

## III. Results: reconstruction of US images

In this section we provide two simulated examples to compare the performance of the proposed BF method with DAS and MV, in terms of lateral resolution, contrast and sidelobe levels. The first one is based on a sparse assumption of the sources. The second one, more realistic, represents the simulation of a cardiac image (the amplitudes of the scatterers were related to the grey levels of an Apical 4 Chambers (A4C) view *in-vivo* image), as suggested in [10]. The raw data for both examples was simulated using the Field II US simulation program [11]. The same simulation parameters, given in the Table I were used for both examples. The display range of the B-mode images was set to 60 dB.

### A. Simulation image of individual scatterers

The resulted images after applying the discussed methods on a sparse medium of only five reflectors are shown in the Fig. 3. In the Fig. 3(a) is the result after applying DAS BF. The lateral resolution is poor and the sidelobes are relatively high. In the Fig. 3(b) MV BF allows the increase of the lateral resolution and the decrease of the sidelobes. Although MV offers better resolution, it still contains high sidelobes. Clearly, Fig. 3(c) presents superiority in terms of high resolution and low sidelobes over DAS and MV BF. This is highlighted by the Fig. 3(d) that illustrates the lateral profiles at the axial

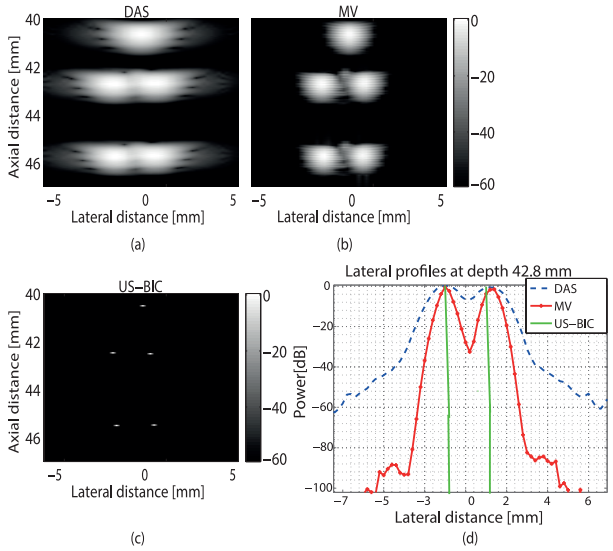


Fig. 3: Comparison between DAS, MV and US-BIC for a sparse medium (the one from the Fig. 2(a)).

depth 42.8 mm of the resulted images using the discussed BF methods.

### B. Simulation of a cardiac apical view in-vivo image

The apical view is very useful in echocardiography, giving information about the ventricle and atrium of the heart. The simulation results are illustrated in Fig. 4, where the left ventricle (LV) is displayed. With this example we investigate the contrast of the aforementioned beamformers. We used the contrast ratio (CR) index and the contrast-to-noise ratio (CNR) to evaluate the contrast resolution of the resulted images. These metrics were computed based on the envelope-detected signals independent of image display range. CR [12] is defined as the ratio of the mean value in the region R1 (represented in the Fig. 4(a) by a white rectangle) to the mean value in the region R2 (represented in the Fig. 4(a) by a black rectangle): $CR = |\mu_{R1} - \mu_{R2}|$. CNR is defined as [13]: $CNR = \frac{CR}{\sqrt{\sigma_{R1}^2+\sigma_{R2}^2}}$, where $\sigma_{R1}$ is the standard deviation of intensities in R1 and $\sigma_{R2}$ the standard deviation of intensities R2.

US-BIC was tested for different values of $\lambda$. As expected, the MV beamformed image from Fig. 4(b) exhibits an overall higher contrast and better resolution than the DAS beamformed image, but not to significant as US-BIC beamformed image.

The values of CR and CNR are presented in the Table II. We can see an improvement of the CR of more than 20 dB compared with DAS and MV. The highest CR and CNR were obtained for $\lambda = 50$. In Fig. 4(c) and Fig. 4(d) we can see that only the most important information is kept, the one related to the interventricular septum (the brightest zone in the image) of the cardiac image. In summary, when we are dealing with some non-sparse medium, $\lambda$ is an important parameter that coordinates the appearance of the final image. Our empirical

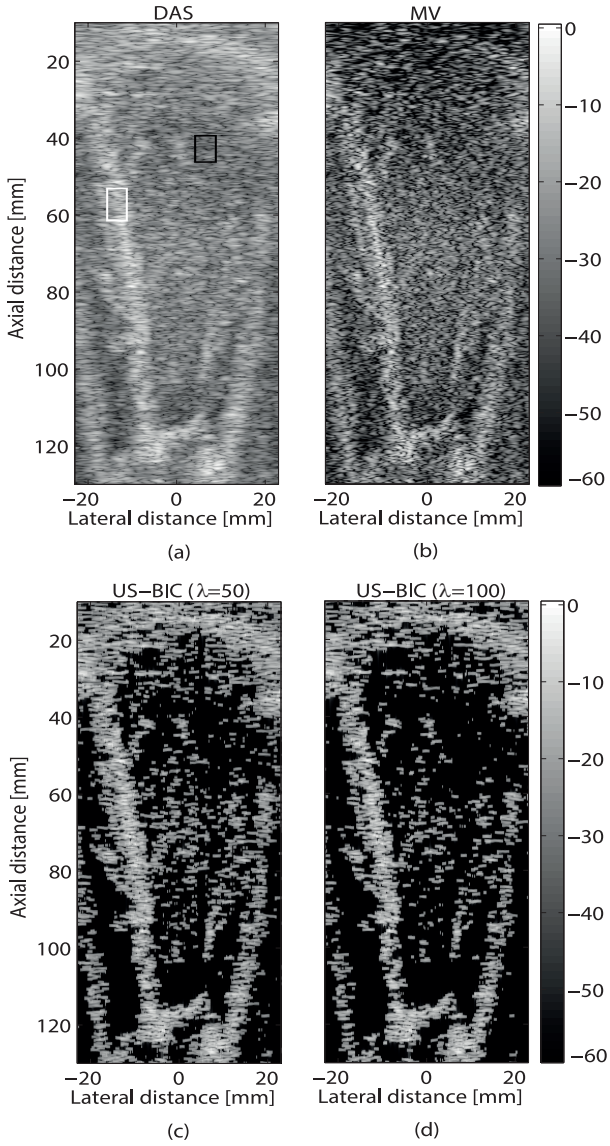


Fig. 4: Results of (a) DAS, (b) MV, (c)-(d) US-BIC BF for different $\lambda$.The values of CNR and CR are given in dB.

experience suggests that in the case of a small value of $\lambda$, the resulted image will be similar with the DAS beamformed image. As much as we increase $\lambda$, less strong reflectors will be detected using US-BIC BF method.

## IV. Conclusion

In this paper we proposed a novel beamforming approach, based on sparse prior of the RF signals. Combining DAS BF with BIC technique, it was shown via numerical experiments that can highly reduce the sidelobes, and increase the spatial resolution and the contrast of the beamformed image. We saw that for sparse scanned medium this method is perfectly detecting the number of present scatterers. For a less sparse medium, the $\lambda$ parameter is deciding how much speckle is filtered out. Independent on the value of $\lambda$, the contrast of the resulted image can be highly improved (a CR of more than 30 dB and a CNR of more than 1 dB) compared with the one of DAS and MV. The proposed approach may be improved by the use of sparse prior in basis such as Fourier [14], or wave atoms [6], or trained dictionaries [15]. Since the term $\lambda$ is established empirical, another improvement can be the development of a method that automatically detects the optimal value of $\lambda$.

TABLE II: CR and CNR values for Fig. 4

| BF Method | CR[dB] | CNR[dB] |
|---|---|---|
| DAS | 13.88 | 1.56 |
| MV | 16.68 | 1.63 |
| US-BIC ($\lambda = 50$) | 51.56 | 2.69 |
| US-BIC ($\lambda = 100$) | 47.87 | 2.16 |

## References


[1] H. L. Van Trees, *Detection, Estimation, and Modulation Theory, Optimum Array Processing*. John Wiley & Sons, 2004.

[2] J. Capon, "High-resolution frequency-wavenumber spectrum analysis," *Proceedings of the IEEE*, vol. 57, no. 8, pp. 1408–1418, 1969.

[3] J.-F. Synnevag, A. Austeng, and S. Holm, "Adaptive beamforming applied to medical ultrasound imaging," *Ultrasonics, Ferroelectrics and Frequency Control, IEEE Transactions on*, vol. 54, no. 8, pp. 1606–1613, 2007.

[4] X. Zeng, Y. Wang, J. Yu, and Y. Guo, "Correspondence-beam-domain eigenspace-based minimum variance beamformer for medical ultrasound imaging," *Ultrasonics, Ferroelectrics and Frequency Control, IEEE Transactions on*, vol. 60, no. 12, pp. 2670–2676, 2013.

[5] B. M. Asl and A. Mahloojifar, "A low-complexity adaptive beamformer for ultrasound imaging using structured covariance matrix," *Ultrasonics, Ferroelectrics and Frequency Control, IEEE Transactions on*, vol. 59, no. 4, pp. 660–667, 2012.

[6] H. Liebgott, A. Basarab, D. Kouame, O. Bernard, and D. Friboulet, "Compressive sensing in medical ultrasound," in *Ultrasonics Symposium (IUS), 2012 IEEE International*. IEEE, 2012, pp. 1–6.

[7] M. Schiffner, T. Jansen, and G. Schmitz, "Compressed sensing for fast image acquisition in pulse-echo ultrasound," *Biomedical Engineering/Biomedizinische Technik*, 2012.

[8] R. Tur, Y. C. Eldar, and Z. Friedman, "Innovation rate sampling of pulse streams with application to ultrasound imaging," *Signal Processing, IEEE Transactions on*, vol. 59, no. 4, pp. 1827–1842, 2011.

[9] S. Konishi and G. Kitagawa, "Bayesian information criteria," *Information Criteria and Statistical Modeling*, pp. 211–237, 2008.

[10] M. Alessandrini, H. Liebgott, D. Friboulet, and O. Bernard, "Simulation of realistic echocardiographic sequences for ground-truth validation of motion estimation," in *Image Processing (ICIP), 2012 19th IEEE International Conference on*. IEEE, 2012, pp. 2329–2332.

[11] J. A. Jensen, "Simulation of advanced ultrasound systems using field ii," in *Biomedical Imaging: Nano to Macro, 2004. IEEE International Symposium on*. IEEE, 2004, pp. 636–639.

[12] S. Flax and M. O'Donnell, "Phase-aberration correction using signals from point reflectors and diffuse scatterers: Basic principles," *Ultrasonics, Ferroelectrics and Frequency Control, IEEE Transactions on*, vol. 35, no. 6, pp. 758–767, 1988.

[13] J. Garayoa and P. Castro, "A study on image quality provided by a kilovoltage cone-beam computed tomography," *Journal of Applied Clinical Medical Physics*, vol. 14, no. 1, 2013.

[14] C. Quinsac, A. Basarab, and D. Kouamé, "Frequency domain compressive sampling for ultrasound imaging," *Advances in Acoustics and Vibration*, vol. 2012, 2012.

[15] O. Lorintiu, H. Liebgott, M. Alessandrini, O. Bernard, and D. Friboulet, "Compressed sensing reconstruction of 3d ultrasound data using dictionary learning," in *IEEE International Conference on Image Processing (ICIP'14)*, 2014, p. accepted.